mathematics

MDPI

Article

Generalized Exp-Function Method to Find Closed Form Solutions of Nonlinear Dispersive Modified Benjamin–Bona–Mahony Equation Defined by Seismic Sea Waves

Muhammad Shakeel [1,†], Attaullah [1], Essam Roshdy El-Zahar [2,3], Nehad Ali Shah [4,*,†] and Jae Dong Chung [4]

[1] Department of Mathematics, University of Wah, Wah Cantt 47040, Pakistan; muhammad.shakeel@uow.edu.pk (M.S.); attaullahsial275@gmail.com (A.)
[2] Department of Mathematics, College of Science and Humanities in Al-Kharj, Prince Sattam Bin Abdulaziz University, P.O. Box 83, Al-Kharj 11942, Saudi Arabia; er.elzahar@psau.edu.sa
[3] Department of Basic Engineering Science, Faculty of Engineering, Menoufia University, Shebin El-Kom 32511, Egypt
[4] Department of Mechanical Engineering, Sejong University, Seoul 05006, Korea; jdchung@sejong.ac.kr
* Correspondence: nehadali199@yahoo.com
† These authors contributed equally to this work.

Abstract: Using the new generalized exp-function method, we were able to derive significant novel closed form solutions to the nonlinear dispersive modified Benjamin–Bona–Mahony (DMBBM) equation. The general framework of the new generalized exp-function method has been given. Many novel closed form solutions have been obtained in the form of hyperbolic, trigonometric, and rational function solutions. Using the computer application Wolfram Mathematica 10, we plotted 2D, 3D, and contour surfaces of closed form solutions found in this work. In the form of a table, the acquired results are compared to the known solutions in the existing literature.

Keywords: generalized exp $(-\phi(\eta))$ expansion method; exact solutions; nonlinear dispersive modified Benjamin–Bona–Mahony equation

MSC: 83C15; 35A20; 35C05; 35C07; 35C08

check for updates

Citation: Shakeel, M.; Attaullah; El-Zahar, E.R.; Shah, N.A.; Chung, J.D. Generalized Exp-Function Method to Find Closed Form Solutions of Nonlinear Dispersive Modified Benjamin–Bona–Mahony Equation Defined by Seismic Sea Waves. *Mathematics* **2022**, *10*, 1026. https://doi.org/10.3390/math10071026

Academic Editor: James M. Buick

Received: 3 March 2022
Accepted: 21 March 2022
Published: 23 March 2022

1. Introduction

Because of their importance in marine ecology, marine geology, and coastal engineering, interest in nonlinear internal solitary waves (ISWs) that occur in the coastal ocean has grown dramatically in recent decades. ISWs frequently have enormous amplitudes and powerful currents; for example, Huang et al. [1] observed an extreme ISW in the northern South China Sea with an amplitude of 240 m and a peak westward current velocity of 2.55 m s^{-1}. Because of the size of these waves, they could pose a risk to undersea drilling. Furthermore, the horizontal propagation of these internal waves provides a mechanism for the movement of energy and momentum over long distances. Internal waves in the coastal ocean are usually studied using the Korteweg–De Vries (KdV) equation, which incorporates cumulative and competing nonlinear and dispersive effects [2].

Although existing Kadomtsev–Petviashvili (KP)-type equations for internal waves can take into account one or more of the impacts of rotation, background current, variable topography, and boundary walls, many of them still rely on model density stratifications, such as a two-layered system. Pierini [3] used the two-layered so-called regularized long-wave equation, a slightly different version of the KP equation, to simulate internal solitary waves in the Alboran Sea under a few simple assumptions, including no background rotation, constant topography, constant interface depth, and no background current. Cai and Xie [4] used a similar model, this time in a two-layered fluid structure, to explore the propagation of ISWs in the northern South China Sea. Despite the two-layered model's apparent simplicity and widespread acceptance, the oceanic density stratification is better represented as continuous when considering oceanic scenarios [5].

A large, seismically produced ocean wave is equipped for extensive destruction in certain waterfront regions, particularly where submarine earthquakes happen. Although in the open ocean the wave height may be short of one meter, it steepens to heights of 15 m or more upon entering shallow seaside water. The frequency in the open sea is in the order of 100 to 150 km, and the rate of movement of a seismic ocean wave is somewhere in the range of 640 and 960 km/h. During recent years, the world has seen a booming number of genuine realities, such as sea acoustic and tsunami wave fields created by earthquakes known to have occurred along the coast of Japan in 2011, generally identified with short-distance seismic activities (earthquakes from Mw 6.9 on 8.8). For example, an investigation studied the first confirmations of natural calamities which were specifically "introduced by Chunga and Toulkeridis [6] the first proof of aleo-tsunami wave stores of the significant memorable occasion in Ecuador". As with seismic ocean waves, the wave length or the height and frequency ranges are vital in terms of creating disasters. These giant forces can be transformed into other energy sources, which will be required soon if fundamental measures are taken. In particular, a few such massive natural tragedies are environment or weather changes and the worldwide temperature warning seen recently. Today, flooding, heat waves, shifting seasons, the fading of coral reefs, rising ocean levels, melting glaciers, and the spread of disease are clear confirmations of environmental changes.

Nonlinear partial deferential equations (NPDEs) have been extensively used in recent years to designate many significant phenomena and dynamic developments in physics, chemistry, mechanics, biology, and many other fields as well. Many powerful methodologies have been developed as a result of the development of soliton theory. For example, the (G′/G)-expansion method [7,8], the sine cosine method [9], the tanh-coth method [10], the F-expansion method [11], the exp-function method [12], the generalized exp-function method [13], and the exp $(-\phi\ (\xi))$ expansion method [14,15]. Fei and Cao [16] used the truncated Painlevé expansion and the CTE method to construct the residual symmetry and the explicit soliton–cnoidal wave interaction solutions for the (2 + 1)-dimensional negative-order breaking soliton equation. Wang et al. [17] used the new scheme by combining the modified Riemann–Liouville fractional derivative rule and two kinds of fractional dual-function methods with the Mittag-Leffler function on the space–time fractional Fokas–Lenells equation to find some new exact analytical solutions including bright soliton, dark soliton, combined soliton, and periodic solutions. Wen et al. [18] used tapered graded-index waveguides with parity–time-symmetric potentials to obtain the light bullet. Fang et al. [19] applied the physics-informed neural network to solve a variety of femtosecond optical soliton solutions of the high-order nonlinear Schrödinger equation, including the one-soliton solution, two-soliton solution, rogue wave solution, W-soliton solution, and M-soliton solution. The Darboux transformation method was used by Raghuraman et al. [20] to obtain a one-soliton solution for the nonlinear Schrödinger equation with a variable dispersion coefficient and an external harmonic potential.

The exp $(-\phi(\eta))$-expansion method is effective for solving NPDEs and can lead to numerous previously unknown closed form solutions. The goal of this work is to generate many new and more general closed form solutions. To that end, we propose a novel generalized approach to investigate NLEEs based on the exp $(-\phi(\eta))$-expansion method. To demonstrate the effectiveness and benefits of this method, we apply it to the nonlinear DMBBM equation.

The generalized exp-function method was successfully applied to the nonlinear DMBBM equation defined as follows:

$$U_t + U_x - \beta\, U^2\, U_x + U_{xxx} \ = 0, \tag{1}$$

where β nonzero and real constant. The nonlinear DMBBM equation was first developed to describe estimation for surface wave propagation in nonlinear dispersive media, but it also categorizes hydromagnetic waves in plasmas, acoustic waves in distinctive form crystals, and acoustic gravitational waves in compressible fluids [21–23]. The modified simple equation (MSE) method was applied by Khan et al. [23] to find exact travelling wave solutions of the nonlinear DMBBM equation and coupled Klein–Gordon equations. Filiz and Arzu [24] utilized the consistent Riccati expansion method for erecting new exact solutions of mKdV-Burgers equations and nonlinear DMBBM equation. The sinh-Gordon function method was used by Yokus et al. [25] to check the stability analysis to find numerical and new closed form trigonometric function solutions of nonlinear DMBBM equation. They used appropriate parameters to perform numerical simulations of the obtained solutions. They also used the finite forward difference approach to solve the exact and numerical approximations of the nonlinear dispersive modified Benjamin–Bona–Mahony equation. They also used the Fourier-Von Neumann analysis to assess the numerical scheme's stability. They displayed the results in the form of a table for both numerical and precise solutions. The error norms were determined by using L_2 and L_∞.

Khater et al. [26] used the modified Khater method to study the computational solutions to the modified Benjamin–Bona–Mahony (BBM) equation. They also looked at the stability of the obtained solutions using the Hamiltonian system's features, evaluating the initial and boundary conditions that allow them to use B-spline collection schemes (cubic, quantic, and septic) to find numerical solutions for the proposed model and explain the similarities between them. The modified exp-function method was applied by Baskonus and Bulut [27] on a nonlinear DMBBM equation to obtain some new exact solutions.

The motivation for this article is to find new and more general solutions to Equation (1). The main novelty of this paper is as follows: (i) the nonlinear DMBBM equation is firstly studied using the generalized exp-function method; (ii) different types of solutions, including rational, exponential, trigonometric, and hyperbolic are obtained. The obtained solutions are compared in the form of Table 1 with the previous results obtained by Baskonus and Bulut [27]. Previous results are re-derived, which shows that our solutions are new and more general. The hyperbolic function solutions, as seen in Figures 1–3, provide physical interpretations of analytical solutions discovered in this study, such as amplitude and widths of seismic sea waves. These hyperbolic function solutions, in other words, show wave length and frequency, as seen in Equations (22), (25), and (28), respectively. The more that wave lengths increase, the more harmful they become all over the globe.

Table 1. Comparison between our solutions and Baskonus and Bulut [27] solutions.

Our Solutions	Baskonus and Bulut [27]
If we put in $A_1 = 1,\ A_2 = 0,\ A_3 = 0,\ A_4 = 1,\ \beta = 1,\ k_1 = 1,\ k_2 = 1, \eta = \xi,\ A = 1$, and $U_1(x,t) = u_1(x,t)$ in Equation (22), then $u_1(x,t) = -2\sqrt{3} + \frac{\sqrt{6}}{\sqrt{2}+\tanh\,(x+t+E)}$.	If we put $\alpha = 1,\ c = -1$, and $\mu = 1$ in Equation (21), then $u_1(x,t) = -2\sqrt{3} + \frac{\sqrt{6}}{\sqrt{2}+\tanh\,(x+t+E)}$.
If we put in $A_1 = 1,\ A_2 = 0,\ A_3 = 0,\ A_4 = 1,\ \beta = 1,\ k_1 = 1, k_2 = -3, \eta = \xi,\ A = 1$, and $U_2(x,t) = u_2(x,t)$ in Equation (23), then $u_2(x,t) = -\frac{\sqrt{6}}{\tan\,(x-3t+E)}$.	If we put $\alpha = 1,\ c = 3$,and$\mu = 1$ in Equation (22), then $u_2(x,t) = -\frac{\sqrt{6}}{\tan\,(x-3t+E)}$.
If we put in $A_1 = 1,\ A_2 = 0,\ A_3 = 0,\ A_4 = 1,\ \beta = 1,\ k_1 = 1, k_2 = -1, \eta = \xi,\ A = 1$, and $U_3(x,t) = u_3(x,t)$ in Equation (24), then $u_3(x,t) = -\frac{\sqrt{6}}{(x-t+E)+1}$.	If we put $\alpha = 1,\ c = 1$, and $\mu = 1$ in Equation (23), then $u_3(x,t) = -\frac{\sqrt{6}}{(x-t+E)+1}$.
If we put in $A_1 = 1,\ A_2 = 0,\ A_3 = 0,\ A_4 = 1,\ \beta = 1,\ k_1 = 1, k_2 = 1, \eta = \xi,\ B = 1$, and $U_4(x,t) = u_4(x,t)$ in Equation (25), then $u_4(x,t) = -\frac{\sqrt{6}}{2} - \frac{3\sqrt{6}}{4\tanh\,(x+t+E)+2}$.	If we put $\alpha = 1,\ c = -1$, and $\lambda = 1$ in Equation (24), then $u_4(x,t) = -\frac{\sqrt{6}}{2} - \frac{3\sqrt{6}}{4\tanh\,(x+t+E)+2}$.

Table 1. *Cont.*

Our Solutions	Baskonus and Bulut [27]
If we put in $A_1 = 1$, $A_2 = 0$, $A_3 = 0$, $A_4 = 1$, $\beta = 1$, $k_1 = 1$, $k_2 = -3, \eta = \xi$, $B = 1$, and $U_5(x,t) = u_5(x,t)$ in Equation (26), then $u_5(x,t) = -\frac{\sqrt{6}}{2} - \frac{5\sqrt{6}}{4\tan(x-3t+E)-2}$.	If we put $\alpha = 1$, $c = 3$, and $\lambda = 1$ in Equation (25), then $u_5(x,t) = -\frac{\sqrt{6}}{2} - \frac{5\sqrt{6}}{4\tan(x-3t+E)-2}$.
If we put in $A_1 = 1$, $A_2 = 0$, $A_3 = 0$, $A_4 = 1$, $\beta = 1$, $k_1 = 1$, $k_2 = -1, \eta = \xi$, $B = 1$, and $U_6(x,t) = u_6(x,t)$ in Equation (27), then $u_6(x,t) = -\frac{\sqrt{6}}{(x-t+E)+2}$.	If we put $\alpha = 1$, $c = 1$, and $\lambda = 1$ in Equation (26), then $u_6(x,t) = -\frac{\sqrt{6}}{(x-t+E)+2}$.
If we put in $A_1 = 1$, $A_2 = 0$, $A_3 = 0$, $A_4 = 1$, $\beta = 1$, $k_1 = 1$, $k_2 = 1, \eta = \xi$, $a_0 = 2$, and $U_7(x,t) = u_7(x,t)$ in Equation (28), then $u_7(x,t) = 2 + \frac{\sqrt{6}}{\sqrt{6}+3\tanh(x+t+E)}$.	If we put $\alpha = 1$, $c = -1$, and $A_0 = 2$ in Equation (27), then $u_7(x,t) = 2 + \frac{\sqrt{6}}{\sqrt{6}+3\tanh(x+t+E)}$.
If we put in $A_1 = 1$, $A_2 = 0$, $A_3 = 0$, $A_4 = 1$, $\beta = 1$, $k_1 = 1$, $k_2 = -3, \eta = \xi$, $a_0 = 2$, and $U_8(x,t) = u_8(x,t)$ in Equation (29), then $u_8(x,t) = 2 + \frac{5\sqrt{6}}{3\tan(x-3t+E)-\sqrt{6}}$.	If we put $\alpha = 1$, $c = 3$, and $A_0 = 2$ in Equation (28), then $u_8(x,t) = 2 + \frac{5\sqrt{6}}{3\tan(x-3t+E)-\sqrt{6}}$.
If we put in $A_1 = 1$, $A_2 = 0$, $A_3 = 0$, $A_4 = 1$, $\beta = 1$, $k_1 = 1$, $k_2 = -1, \eta = \xi$, and $U_9(x,t) = u_9(x,t)$ in Equation (30), then $u_9(x,t) = \frac{\sqrt{6}}{\sqrt{6}(x-t+E)+3}$.	If we put $\alpha = 1$, $c = 1$, and $A_0 = 2$ in Equation (29), then $u_9(x,t) = \frac{\sqrt{6}}{\sqrt{6}(x-t+E)+3}$.

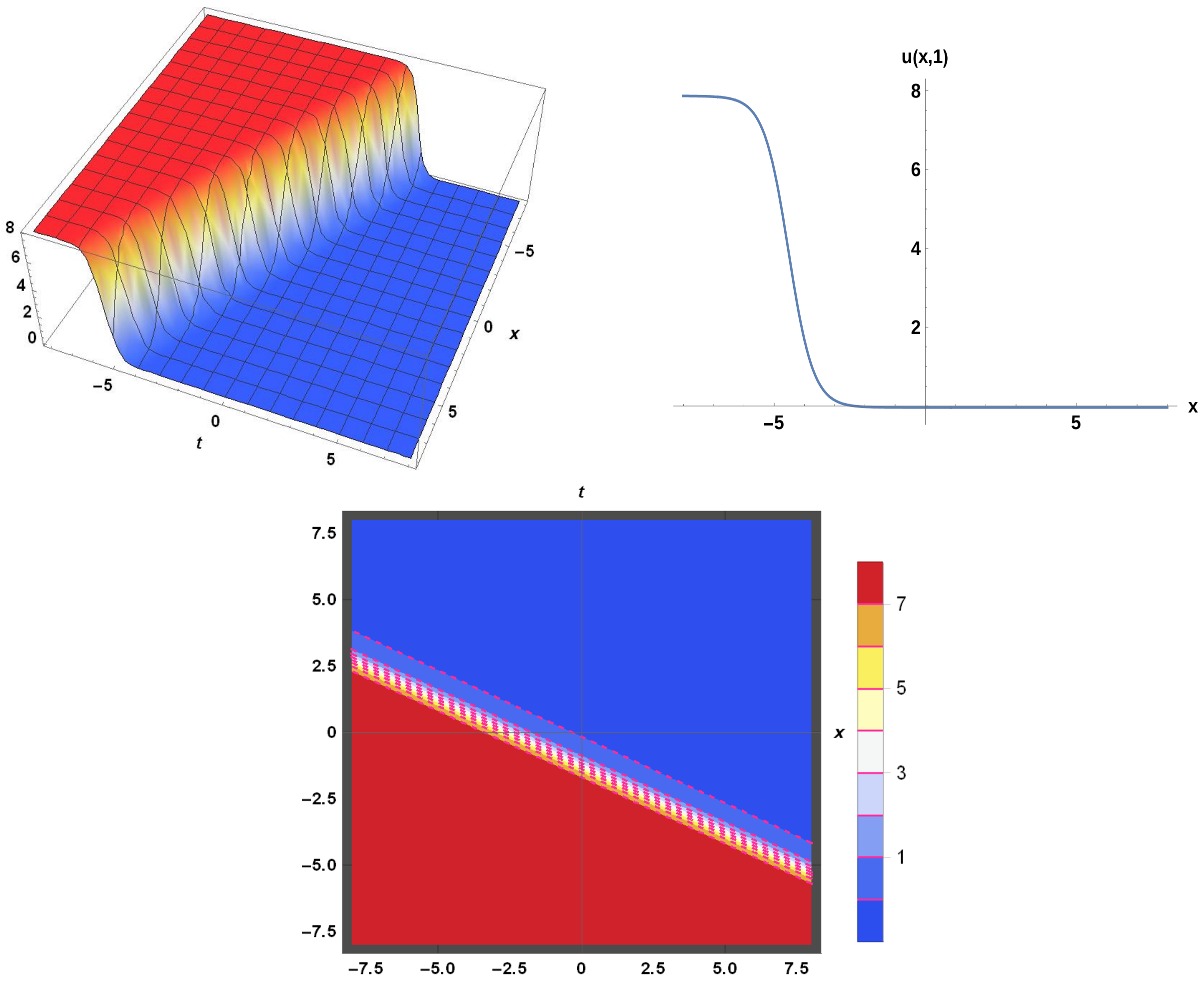

Figure 1. The solitary wave view of the 3D, 2D, and contour plots of $U_1(x,t)$.

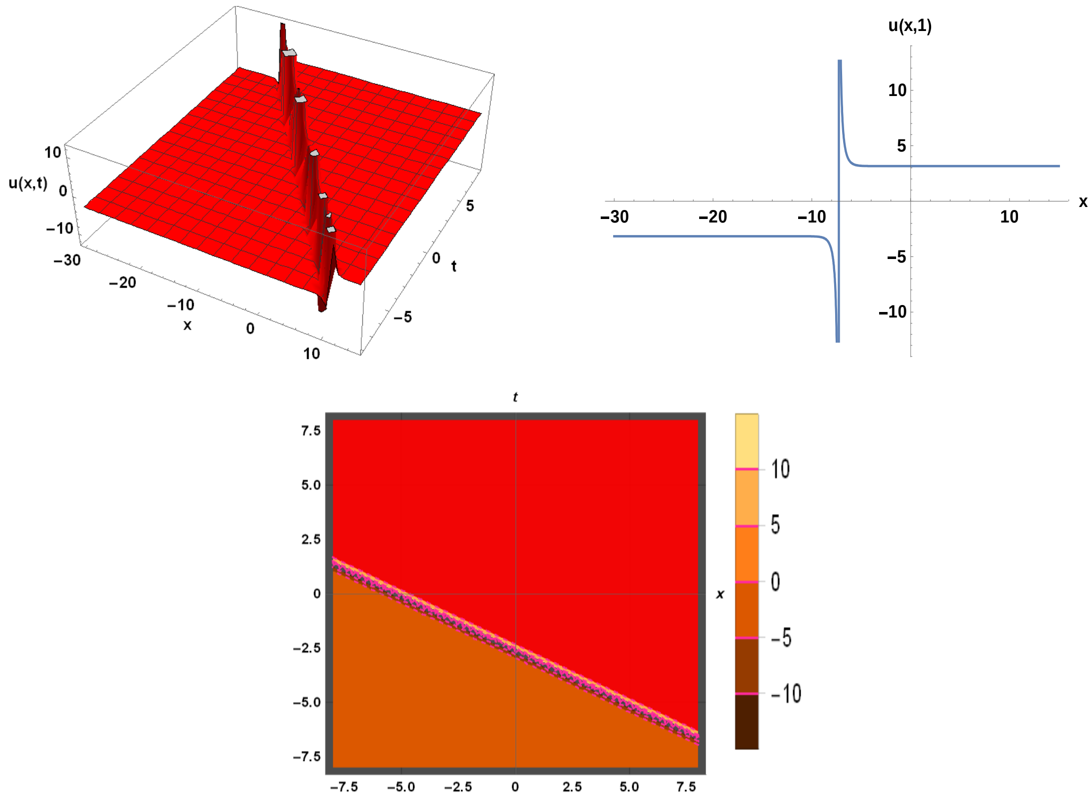

Figure 2. The solitary wave view of the 3D, 2D, and contour plots of $U_2(x, t)$.

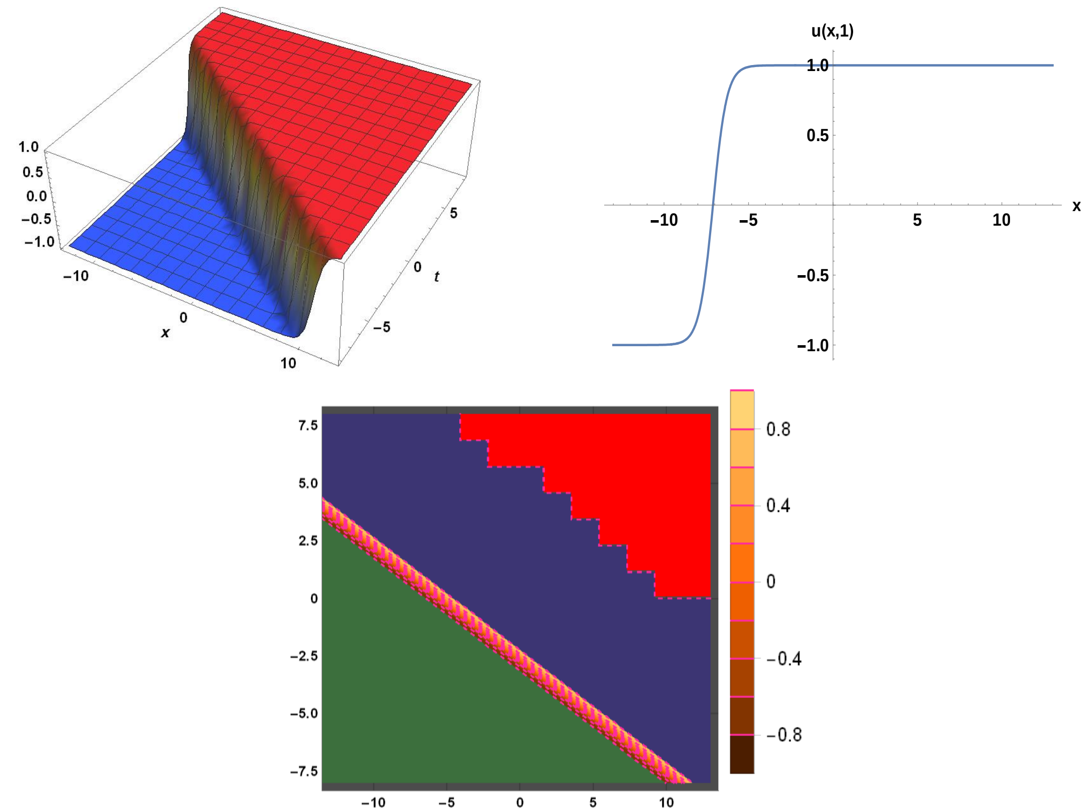

Figure 3. The solitary wave view of the 3D, 2D, and contour plots of $U_3(x, t)$.

2. Description of the Method

Assume we have a nonlinear PDE given below of the form [13]

$$F\,(U,\ U_x,\ U_t,\ U_{x\,x},\ U_{t\,t},\ U_{x\,t},\ U_{x\,x\,t},\ldots)\ =0, \tag{2}$$

where U is an unidentified function, and F is a polynomial in U and its derivatives with respect to x and t, which includes derivatives of highest-order and nonlinear terms. The major steps of the generalized exp-function method are:

Step 1: The travelling wave transformation:

$$U(x,t) = U\,(\eta), \quad \eta = k_1\,x + k_2\,t, \tag{3}$$

where k_1 and k_2 are constants to be found later, and Equation (2) is transformed into an ordinary differential equation (ODE):

$$P\big(U,\ k_1U',\ k_2U',\ k_1k_2U'',\ldots\big) = 0. \tag{4}$$

Step 2: Assume the trial solution of Equation (4) can be written as:

$$U\,(\eta)\ =\ \sum_{\mathrm{i}=0}^{m} a_i\,\left[\exp\left(-\frac{A_1\,\phi\,(\eta)\ +A_2}{A_3\,\phi\,(\eta)\ +A_4}\right)\right]^{\mathrm{i}}, \tag{5}$$

where $a_i,\ a_m \neq 0,\ (0 \le i \le m)$ are undetermined constants and $\phi\,(\eta)$ satisfies the following differential equation:

$$\phi'(\eta)\ =\ \frac{(A_3\,\phi\,(\eta)\ +A_4)^2}{(A_1\,A_4\ +A_2\,A_3)}\left(\exp\left(-\frac{A_1\,\phi\,(\eta)\ +A_2}{A_3\,\phi\,(\eta)\ +A_4}\right)+A\exp\left(\frac{A_1\,\phi\,(\eta)\ +A_2}{A_3\,\phi\,(\eta)\ +A_4}\right)+B\right), \tag{6}$$

where $\Delta = (A_1\,A_4\ -A_2\,A_3) \neq\ 0$. Equation (6) has the following families of solutions:

Family 1: When $\Delta = (A_1\,A_4\ -A_2\,A_3) \neq\ 0,\ A \neq 0,\ \big(B^2 - 4A\ \big)\ > 0, A_2\ = 0$,

$$\phi_1(\eta)\ =\ \frac{A_4\ \ln\left(\frac{-\sqrt{B^2-4A}\,\tanh\left(\frac{\sqrt{B^2-4A}}{2}(\eta+E)\right)-B}{2A}\right)}{A_1 - A_3\ln\left(\frac{-\sqrt{B^2-4A}\,\tanh\left(\frac{\sqrt{B^2-4A}}{2}(\eta+E)\right)-B}{2A}\right)} \tag{7}$$

Family 2: When $\Delta = (A_1\,A_4\ -A_2\,A_3) \neq\ 0,\ A \neq 0, \big(B^2 - 4A\ \big)\ < 0,\ A_2\ = 0$,

$$\phi_2(\eta)\ =\ \frac{A_4\ \ln\left(\frac{\sqrt{-B^2+4A}\ \tan\left(\frac{\sqrt{-B^2+4A}}{2}(\eta+E)\right)-B}{2A}\right)}{A_1 - A_3\ln\left(\frac{\sqrt{-B^2+4A}\ \tan\left(\frac{\sqrt{-B^2+4A}}{2}(\eta+E)\right)-B}{2A}\right)} \tag{8}$$

Family 3: When $\Delta = (A_1\,A_4\ -A_2\,A_3) \neq\ 0,\ A\ \neq 0,\ B\ \neq 0, \big(B^2 - 4A\ \big) = 0,\ A_2\ = 0$,

$$\phi_3(\eta)\ =\ \frac{A_4\ \ln\left(-\frac{2(B(\eta+E))+2}{B^2\ (\eta+E)}\right)}{A_1 - A_3\ln\ \left(-\frac{2\ (B(\eta+E))+2}{B^2\ (\eta+E)}\right)}. \tag{9}$$

Family 4: When $\Delta = (A_1\,A_4\ -A_2\,A_3) \neq\ 0,\ A\ \neq 0,\ B\ \neq 0, \big(B^2 - 4A\ \big)\ > 0, A_3\ = 0$,

$$\phi_4(\eta) = -2\left(\frac{A_2}{A_1}\right) + \left(\frac{A_4}{A_1}\right)\ln\left(\frac{-\tanh\left(\sqrt{(B^2-4A)}\frac{(\eta+E)}{2}\right)\sqrt{e^{\left(\frac{2A_2}{A4}\right)}(B^2-4A)} - Be^{\left(\frac{A_2}{A_4}\right)}}{2A}\right). \quad (10)$$

Family 5: When $\Delta = (A_1\, A_4 - A_2\, A_3) \neq 0, A \neq 0, B \neq 0, (B^2 - 4A) < 0, A_3 = 0,$

$$\phi_5(\eta) = -2\left(\frac{A_2}{A_1}\right) + \left(\frac{A_4}{A_1}\right)\ln\left(\frac{-\tan\left(\sqrt{(-B^2+4A)}\frac{(\eta+E)}{2}\right)\sqrt{e^{\left(\frac{2A_2}{A4}\right)}(-B^2+4A)} - Be^{\left(\frac{A_2}{A_4}\right)}}{2A}\right) \quad (11)$$

Family 6: When $\Delta = (A_1\, A_4 - A_2\, A_3) \neq 0, A \neq 0, B \neq 0, (B^2 - 4A) = 0, A_3 = 0,$

$$\phi_6(\eta) = -\left(\frac{A_2}{A_1}\right) + \left(\frac{A_4}{A_1}\right)\ln\left(\frac{2(B(\eta+E)+2)}{B^2(\eta+E)}\right) \quad (12)$$

Family 7: When $\Delta = (A_1\, A_4 - A_2\, A_3) \neq 0, A = 0, B \neq 0, (B^2 - 4A) > 0,$

$$\phi_7(\eta) = -\left(\frac{A_2 + A_4\ln\left(\frac{B}{\exp(B(\eta+E))-1}\right)}{A_1 + A_3\ln\left(\frac{B}{\exp(B(\eta+E))-1}\right)}\right) \quad (13)$$

Family 8: When $\Delta = (A_1\, A_4 - A_2\, A_3) \neq 0, A = 0, B = 0, (B^2 - 4A) = 0,$

$$\phi_8(\eta) = -\frac{A_2 - A_4\ln(\eta+E)}{A_1 - A_3\ln(\eta+E)}. \quad (14)$$

Family 9: When $(A_1\, A_4 - A_2\, A_3) \neq 0, A \neq 0, B \neq 0, (B^2 - 4A) = 0, A_{\mathrm{i}} \neq 0 (i = 1, 2, 3, 4),$

$$\phi_9(\eta) = -\frac{A_2 - A_4\ln\left(-\frac{2(\eta+E)}{B(\eta+E)-2}\right)}{A_1 - A_3\ln\left(-\frac{2(\eta+E)}{B(\eta+E)-2}\right)}. \quad (15)$$

Family 10: When $\Delta = (A_1\, A_4 - A_2\, A_3) \neq 0, A < 0, B = 0,$

$$\phi_{10}(\eta) = -\frac{A_2 - A_4\ln\left(-\frac{\exp\left(-2\sqrt{-A}(\eta+E)\right)+1}{\sqrt{-A}\,\exp\left(-2\sqrt{-A}(\eta+E)\right)-1}\right)}{A_1 - A_3\ln\left(-\frac{\exp\left(-2\sqrt{-A}(\eta+E)\right)+1}{\sqrt{-A}\,\exp\left(-2\sqrt{-A}(\eta+E)\right)-1}\right)}. \quad (16)$$

Step 3: We calculate the value of the positive integer m by using the balancing principle between the highest-order derivative and the highest-order nonlinear term in Equation (4).

Step 4: Swapping Equation (5) into Equation (4) and then using Equation (6), and setting all the coefficients of $\left[\exp\left(-\frac{A_1\,\phi\,(\eta)\,+A_2}{A_3\,\phi\,(\eta)\,+A_4}\right)\right]^i$ to the zero, yields a system of the algebraic equations for $k_1,\ A,\ B,\ k_2$ and (i = 0, 1, 2, 3, … m). The values of the constants $k_1,\ A,\ B,\ k_2$ and a_i $(i = 0,\ 1,\ 2, \ldots, m)$ can be determined by solving the algebraic system of equations. Because the general solutions of (6) are known to us, we can substitute $k_1,\ k_2,\ B,\ A$ and a_i as well as the general solutions of (6) into Equation (5) to obtain the exact solutions of nonlinear PDEs (1).

3. Applications

In this section, we obtain new closed form solutions with the application of the generalized exp $(-\phi(\eta))$-expansion method to the nonlinear DMBBM equation.

The travelling wave variable Equation (3), converts Equation (1) to the following nonlinear ordinary differential equation:

$$U'(\eta)\,k_2 + U'(\eta)\,k_1 + U'''(\eta)\,k_1^3 - \beta\,U(\eta)^2\,\left(U'(\eta)\right)k_1 = 0. \tag{17}$$

where β, k_1, and k_2 are nonzero real constants.

By balancing principle between U''' and U^2U'' in (17), we get m = 1. As a result, the trial solution (5) becomes:

$$U(\eta) = a_0 + a_1\,\exp\left(-\frac{A_1\,\phi(\eta) + A_2}{A_3\,\phi(\eta) + A_4}\right). \tag{18}$$

Switching Equation (18) along with Equation (6) into Equation (17), we get a polynomial in $\left(\exp\left(-\frac{A_1\,\phi(\eta)+A_2}{A_3\,\phi(\eta)+A_4}\right)\right)^j$, $(j = 0,\,1,\,2,\,\ldots)$, and then equate all the coefficients of the resulting polynomial to zero, yielding a set of the simultaneous algebraic equations for a_0, a_1, k_1, k_2, B, A, and β. After solving the algebraic system by using Maple 18, we acquire the following values of the coefficients:

Case 1:

$$a_0 = -\frac{\sqrt{3\beta\,k_1\left(2A\,k_1^3 + k_1 + k_2\right)}}{\beta\,k_1},\ a_1 = -\frac{\sqrt{6}\,k_1}{\beta},\ B = \frac{\sqrt{2\beta\,k_1\left(2A\,k_1^3 + k_1 + k_2\right)}}{\beta\,k_1^2}, A = A,\ k_1 = k_1,\ k_2 = k_2. \tag{19}$$

Case 2:

$$a_0 = -\frac{B\,k_1\sqrt{6}}{2\sqrt{\beta}},\ a_1 = -\frac{\sqrt{6}\,k_1}{\beta},\ A = \frac{B^2\,k_1^3 - 2k_1 - 2k_2}{4k_1^3},\ B = B,\ k_1 = k_1,\ k_2 = k_2. \tag{20}$$

Case 3:

$$a_0 = a_0,\ a_1 = \frac{\sqrt{6}\,k_1}{\beta},\ A = \frac{1}{6}\frac{\beta\,a_0^2\,k_1 - 3\,k_1 - 3k_2}{k_1^3},\ B = \frac{1}{3}\frac{\sqrt{\beta}\,a_0\sqrt{6}}{k_1}, k_1 = k_1,\ k_2 = k_2. \tag{21}$$

To begin, the hyperbolic, trigonometric, and rational functions solutions are obtained to the nonlinear DMBBM equation by substituting the value of coefficients from Equation (19) into Equation (18) together with examining Equations (7)–(9) as follows, respectively:

$$U_1(x,t) = -\frac{\sqrt{3\beta\,k_1\left(2A\,k_1^3 + k_1 + k_2\right)}}{\beta\,k_1} - \frac{\sqrt{6}\,k_1}{\beta}\,\exp\left(-\frac{A_1\,\dfrac{A_4\,\ln\left(\frac{-\sqrt{B^2-4A}\,\tanh\left(\frac{\sqrt{B^2-4A}}{2}(\eta+E)\right)-B}{2A}\right)}{A_1 - A_3\ln\left(\frac{-\sqrt{B^2-4A}\,\tanh\left(\frac{\sqrt{B^2-4A}}{2}(\eta+E)\right)-B}{2A}\right)} + A_2}{A_3\,\dfrac{A_4\,\ln\left(\frac{-\sqrt{B^2-4A}\,\tanh\left(\frac{\sqrt{B^2-4A}}{2}(\eta+E)\right)-B}{2A}\right)}{A_1 - A_3\ln\left(\frac{-\sqrt{B^2-4A}\,\tanh\left(\frac{\sqrt{B^2-4A}}{2}(\eta+E)\right)-B}{2A}\right)} + A_4}\right). \tag{22}$$

$$U_2(x,t) = -\frac{\sqrt{3\beta\, k_1 \left(2A\, k_1^3 + k_1 + k_2\right)}}{\beta\, k_1} - \frac{\sqrt{6}\, k_1}{\beta}\, \exp\left(-\frac{A_1 \dfrac{A_4 \ln\left(\frac{\sqrt{-B^2+4A}\, \tan\left(\frac{\sqrt{-B^2+4A}}{2}(\eta+E)\right) - B}{2A}\right)}{A_1 - A_3 \ln\left(\frac{\sqrt{-B^2+4A}\, \tan\left(\frac{\sqrt{-B^2+4A}}{2}(\eta+E)\right) - B}{2A}\right)} + A_2}{A_3 \dfrac{A_4 \ln\left(\frac{\sqrt{-B^2+4A}\, \tan\left(\frac{\sqrt{-B^2+4A}}{2}(\eta+E)\right) - B}{2A}\right)}{A_1 - A_3 \ln\left(\frac{\sqrt{-B^2+4A}\, \tan\left(\frac{\sqrt{-B^2+4A}}{2}(\eta+E)\right) - B}{2A}\right)} + A_4} \right). \tag{23}$$

$$U_3(x,t) = -\frac{\sqrt{3\beta\, k_1 \left(2A\, k_1^3 + k_1 + k_2\right)}}{\beta\, k_1} - \frac{\sqrt{6}\, k_1}{\beta}\, \exp\left(-\frac{A_1 \dfrac{A_4 \ln\left(-\frac{2(B(\eta+E))+2}{B^2\,(\eta+E)}\right)}{A_1 - A_3 \ln\left(-\frac{2\,(B(\eta+E))+2}{B^2\,(\eta+E)}\right)} + A_2}{A_3 \dfrac{A_4 \ln\left(-\frac{2(B(\eta+E))+2}{B^2\,(\eta+E)}\right)}{A_1 - A_3 \ln\left(-\frac{2\,(B(\eta+E))+2}{B^2\,(\eta+E)}\right)} + A_4} \right). \tag{24}$$

where $\eta = (\, k_1\, x + k_2\, t\,)$.

Secondly, we calculate the hyperbolic, trigonometric, and rational functions solutions for Equation (1) by substituting the coefficient values from Equation (20) into Equation (18) and considering Equations (7)–(9) as follows:

$$U_4(x,t) = -\frac{B\, k_1 \sqrt{6}}{2\sqrt{\beta}} - \frac{\sqrt{6}\, k_1}{\beta}\, \exp\left(-\frac{A_1 \dfrac{A_4 \ln\left(\frac{-\sqrt{B^2-4A}\, \tanh\left(\frac{\sqrt{B^2-4A}}{2}(\eta+E)\right) - B}{2A}\right)}{A_1 - A_3 \ln\left(\frac{-\sqrt{B^2-4A}\, \tanh\left(\frac{\sqrt{B^2-4A}}{2}(\eta+E)\right) - B}{2A}\right)} + A_2}{A_3 \dfrac{A_4 \ln\left(\frac{-\sqrt{B^2-4A}\, \tanh\left(\frac{\sqrt{B^2-4A}}{2}(\eta+E)\right) - B}{2A}\right)}{A_1 - A_3 \ln\left(\frac{-\sqrt{B^2-4A}\, \tanh\left(\frac{\sqrt{B^2-4A}}{2}(\eta+E)\right) - B}{2A}\right)} + A_4} \right). \tag{25}$$

$$U_5(x,t) = -\frac{B\, k_1 \sqrt{6}}{2\sqrt{\beta}} - \frac{\sqrt{6}\, k_1}{\beta}\, \exp\left(-\frac{A_1 \dfrac{A_4 \ln\left(\frac{\sqrt{-B^2+4A}\, \tan\left(\frac{\sqrt{-B^2+4A}}{2}(\eta+E)\right) - B}{2A}\right)}{A_1 - A_3 \ln\left(\frac{\sqrt{-B^2+4A}\, \tan\left(\frac{\sqrt{-B^2+4A}}{2}(\eta+E)\right) - B}{2A}\right)} + A_2}{A_3 \dfrac{A_4 \ln\left(\frac{\sqrt{-B^2+4A}\, \tan\left(\frac{\sqrt{-B^2+4A}}{2}(\eta+E)\right) - B}{2A}\right)}{A_1 - A_3 \ln\left(\frac{\sqrt{-B^2+4A}\, \tan\left(\frac{\sqrt{-B^2+4A}}{2}(\eta+E)\right) - B}{2A}\right)} + A_4} \right). \tag{26}$$

$$U_6(x,t) = -\frac{B\,k_1\sqrt{6}}{2\sqrt{\beta}} - \frac{\sqrt{6}\,k_1}{\beta}\,\exp\left(-\frac{A_1\,\frac{A_4\,\ln\left(-\frac{2(B(\eta+E))+2}{B^2\,(\eta+E)}\right)}{A_1-A_3\ln\left(-\frac{2\,(B(\eta+E))+2}{B^2\,(\eta+E)}\right)}+A_2}{A_3\,\frac{A_4\,\ln\left(-\frac{2(B(\eta+E))+2}{B^2\,(\eta+E)}\right)}{A_1-A_3\ln\left(-\frac{2\,(B(\eta+E))+2}{B^2\,(\eta+E)}\right)}+A_4}\right). \tag{27}$$

where $\eta = (\,k_1\,x + k_2\,t\,)$.

Lastly, we calculate the hyperbolic, trigonometric, and rational functions solutions for Equation (1) by substituting the coefficient values from Equation (21) into Equation (18) and considering Equations (7)–(9) as follows:

$$U_7(x,t) = a_0 + \frac{\sqrt{6}\,k_1}{\beta}\,\exp\left(-\frac{A_1\,\frac{A_4\,\ln\left(\frac{-\sqrt{B^2-4A}\,\tanh\left(\frac{\sqrt{B^2-4A}}{2}(\eta+E)\right)-B}{2A}\right)}{A_1-A_3\ln\left(\frac{-\sqrt{B^2-4A}\,\tanh\left(\frac{\sqrt{B^2-4A}}{2}(\eta+E)\right)-B}{2A}\right)}+A_2}{A_3\,\frac{A_4\,\ln\left(\frac{-\sqrt{B^2-4A}\,\tanh\left(\frac{\sqrt{B^2-4A}}{2}(\eta+E)\right)-B}{2A}\right)}{A_1-A_3\ln\left(\frac{-\sqrt{B^2-4A}\,\tanh\left(\frac{\sqrt{B^2-4A}}{2}(\eta+E)\right)-B}{2A}\right)}+A_4}\right). \tag{28}$$

$$U_8(x,t) = a_0 + \frac{\sqrt{6}\,k_1}{\beta}\,\exp\left(-\frac{A_1\,\frac{A_4\,\ln\left(\frac{\sqrt{-B^2+4A}\,\tan\left(\frac{\sqrt{-B^2+4A}}{2}(\eta+E)\right)-B}{2A}\right)}{A_1-A_3\ln\left(\frac{\sqrt{-B^2+4A}\,\tan\left(\frac{\sqrt{-B^2+4A}}{2}(\eta+E)\right)-B}{2A}\right)}+A_2}{A_3\,\frac{A_4\,\ln\left(\frac{\sqrt{-B^2+4A}\,\tan\left(\frac{\sqrt{-B^2+4A}}{2}(\eta+E)\right)-B}{2A}\right)}{A_1-A_3\ln\left(\frac{\sqrt{-B^2+4A}\,\tan\left(\frac{\sqrt{-B^2+4A}}{2}(\eta+E)\right)-B}{2A}\right)}+A_4}\right). \tag{29}$$

$$U_9(x,t) = a_0 + \frac{\sqrt{6}\,k_1}{\beta}\,\exp\left(-\frac{A_1\,\frac{A_4\,\ln\left(-\frac{2(B(\eta+E))+2}{B^2\,(\eta+E)}\right)}{A_1-A_3\ln\left(-\frac{2\,(B(\eta+E))+2}{B^2\,(\eta+E)}\right)}+A_2}{A_3\,\frac{A_4\,\ln\left(-\frac{2(B(\eta+E))+2}{B^2\,(\eta+E)}\right)}{A_1-A_3\ln\left(-\frac{2\,(B(\eta+E))+2}{B^2\,(\eta+E)}\right)}+A_4}\right). \tag{30}$$

where $\eta = (\,k_1\,x + k_2\,t\,)$.

Remark: If we put $A_1 = 1, A_2 = 0,\ A_3 = 0,\ A_4 = 1,\ a_0 = A_0,\ a_1 = A_1,\ \phi = \Omega$, and $\eta = \xi$ then our Equation (18) coincides with Equation (15) of Baskonus and Bulut [27].

4. Physical Expression of the Problem

The hyperbolic function solutions as seen in Figures 1–3 provide physical interpretations of analytical solutions discovered in this study, such as amplitude and widths of seismic sea waves. These hyperbolic function solutions, in other words, demonstrate that wave length and frequency is shown in Equations (22), (25), and (28), respectively. The more that wave lengths increase, the more harmful they become all over the globe. We should investigate the mathematical structures of these natural challenges in order to lessen the destructive force of such massive natural disasters or convert them into useful energy sources. We can find the best technique to understand such potential calamities and then take the required countermeasures if we tackle these difficulties by utilizing various methods.

Periodic travelling wave solutions 23, 26, and 29 are one-dimensional space periodic functions, such as $\cos(x - t)$, which move at a constant speed. As a result, there is a unique sort of spatiotemporal oscillation in which both space and time are periodic. Many mathematical equations, such as self-oscillatory systems, excitable systems, and reaction–diffusion–advection systems, rely on periodic travelling waves. These types of equations are commonly utilized in biology, chemistry, and physics as mathematical models. The solutions 24, 27, and 30 represent the singular kink type solitons.

We investigate the nature of the number of solutions obtained by employing the generalized exp-function method to the nonlinear DMBBM equation and specifying specific parameter values. In addition, we provide graphs of the exact solutions generated by the mathematical software Mathematica 10. The entire set of results is depicted in Figures 1–9. As a result of these findings in our paper, we discovered that Equations (21)–(29) exhibit kink-shaped solitons, solitons, periodic solutions, and singular kink type solitons. Figure 1 displays the shape kink types of the exact solutions of 3D, 2D, and contour plots of the hyperbolic function solution of $U_1(x,\ t)$, for the unknown constants $\beta = 0.8$, A = 0.8, $k_1 = 1$, $k_2 = 2$, E = 5, and within the interval $-8 \leq x,\ t \leq 8$ for the 3D graph and t = 1 for the 2D graph. Figure 2 displays the 3D, 2D, and contour plot kink type soliton solutions of $U_2(x,\ t)$ for$\beta = 0.9$, B = 1, $k_1 = 1$, $k_2 = 2$, E = 5, and within the intervals $-18 \leq x \leq 15$, $8 \leq t \leq 8$,for the 3D graph and t = 1 for the 2D graph. The hyperbolic function solution in Figure 3 demonstrates the kink type shape of $U_3(x,\ t)$ for the unknown constants$\beta = 9$,$a_0 = 8$, $k_1 = 1$, $k_2 = 2$, E = 5, to the interval $-13 \leq x \leq 13$, $8 \leq t \leq 8$ for 3D graphs and $t\ =\ 1$ for 2D graphs. Equation (22) represents the exact periodic travelling wave solution. The periodic travelling wave solution of the $U_2(x,\ t)$ and the unknown constants $\beta = 0.9$, A = 8, $k_1 = 1$, $k_2 = -0.8$, E = 5, within the interval $-8 \leq x, t \leq 8$ for the 3D graph and t = 1 for the 2D graph are shown in Figure 4. Figure 5 represents the singular kink wave type travelling wave solution of $U_5(x,\ t)$, for which the constants are $\beta = 0.9$, A = 1, $k_1 = 1$, $k_2 = 1$, E = 5 and between intervals $-18 \leq x \leq 18$, $8 \leq t \leq 8$, for the 3D graph and t = 1 for the 2D graph. Equation (23) is a singular soliton solution. Figure 6 shows 3D, 2D, and contour plots of the trigonometric function solution $U_6(x,\ t)$ that act like the periodic travelling wave solution for the unknown constants $\beta = 0.9$, B = 1, $k_1 = 1$, $k_2 = -2$, E = 5 and between the intervals $-30 \leq x \leq 15$, $8 \leq t \leq 8$ for the 3D graph and t = 10 for the 2D graph. The 3D, 2D, and contour plots of the solution $U_7(x,\ t)$ in Equation (26) behave like a singular kink wave type travelling wave solution for the unknown constants $\beta = 0.9$, B = 0.8, $k_1 = 1$, $k_2 = 1$, E = 5 and to the interval $-18 \leq x \leq 18$, $8 \leq t \leq 8$, for 3D graphs and $t = 1$ for 2D graphs, which are shown in Figure 7. Figure 8 represents the periodic soliton wave solutions to the 3D, 2D, and contour graphs of the trigonometric function solution in $U_8(x,\ t)$ for the different values of the parameters $\beta = 9$, $a_0 = 8$, $k_1 = 1$, $k_2 = -2$, E = 5 within the interval $-13 \leq x \leq 13$, $8 \leq t \leq 8$ for 3D graphs and $t =\ 1$ for the 2D graphs. Figure 9 shows the singular kink travelling wave solution of U_9(x, t) for the unknown constants $\beta = 9$,$a_0 = 8$, $k_1 = 1$, $k_2 = -1$, E = 5 for 3D graphs within the interval of $-8 \leq x \leq 8$, $18 \leq t \leq 18$, and $t = 10$ for the 2D graph. In Figures 1–9, we display the values of the parameters $A_1\ = 1,\ A_2\ = 0,\ \ A_3\ = 0,\ \ A_4\ = 1$.

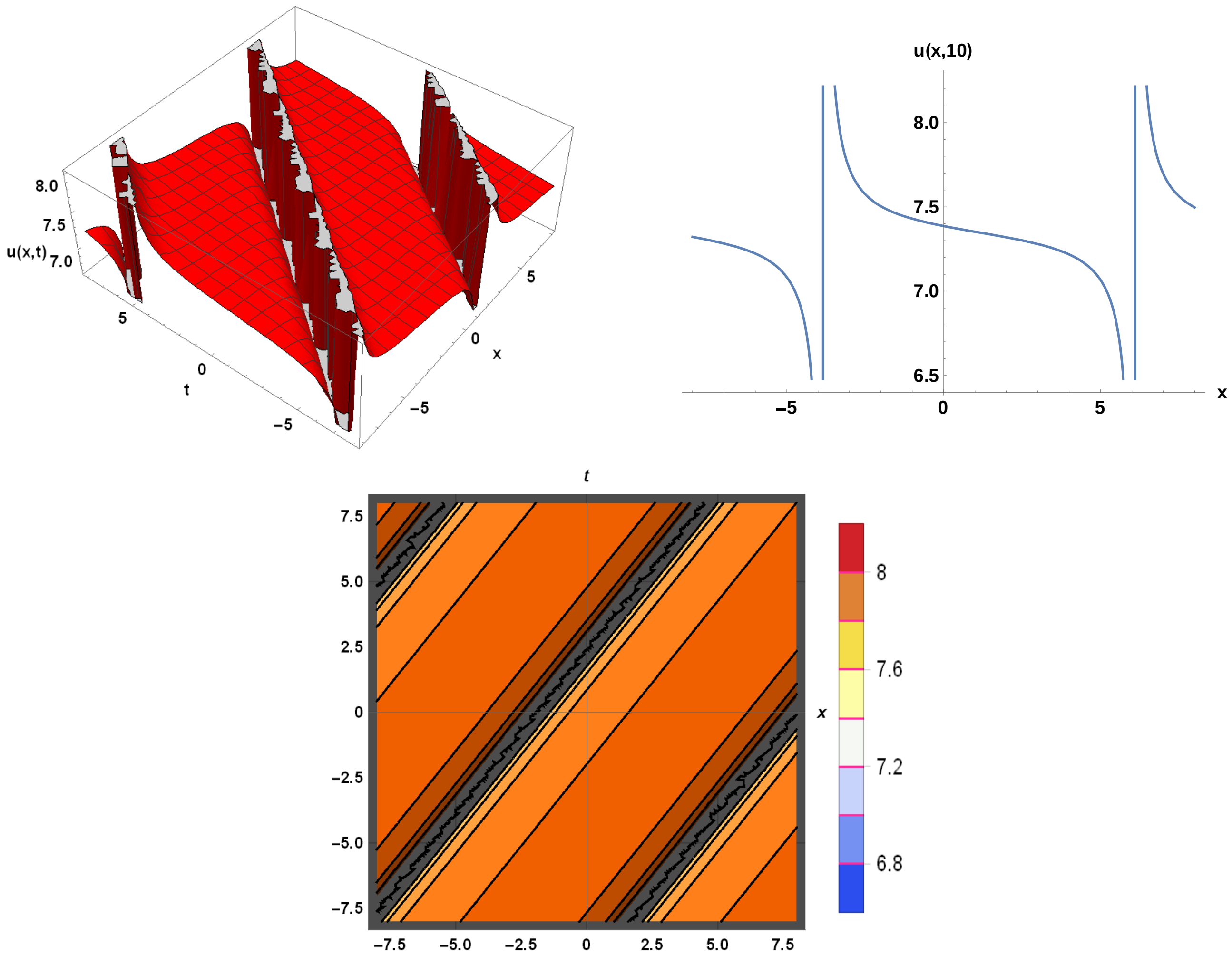

Figure 4. The solitary wave view of 3D, 2D, and contour plots of $U_4(x, t)$.

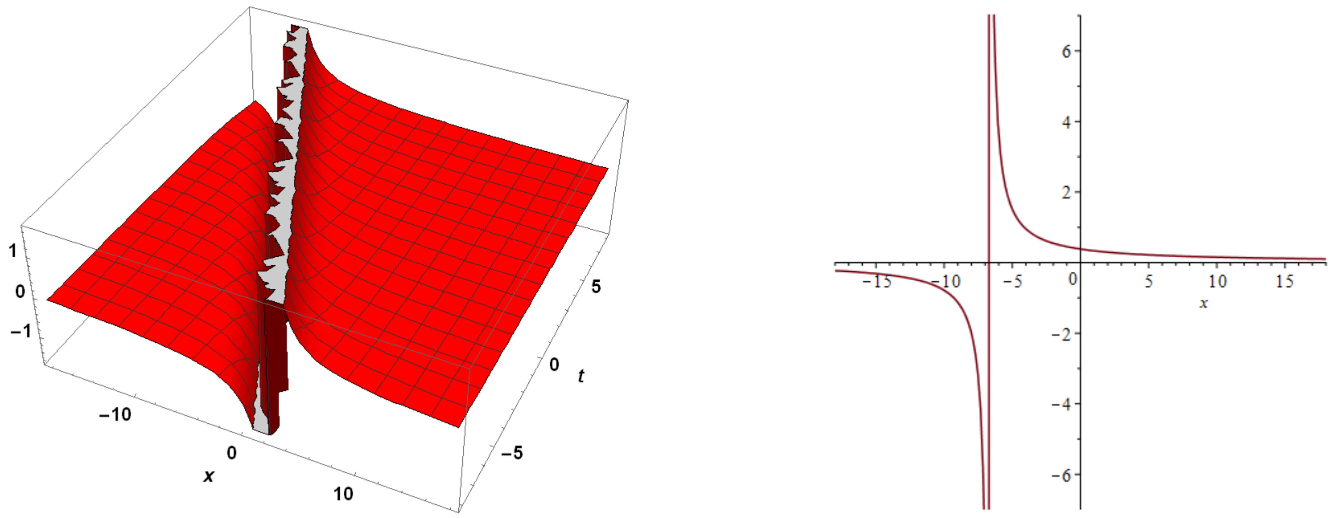

Figure 5. *Cont.*

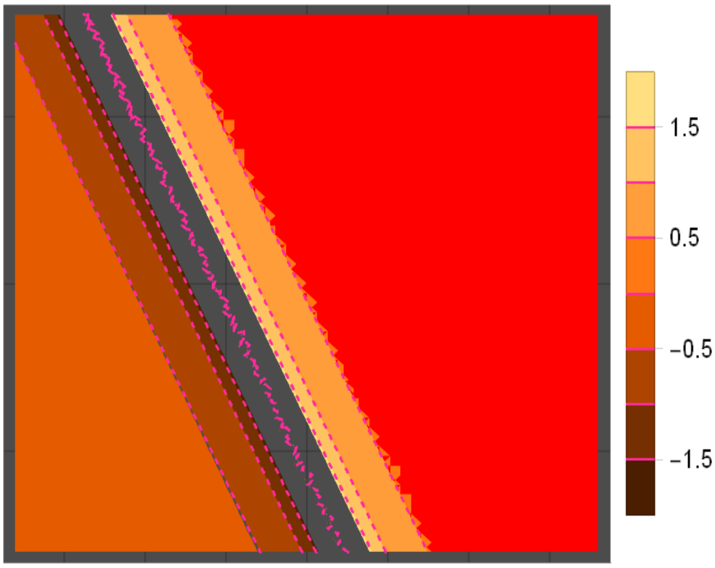

Figure 5. The solitary wave view of the 3D, 2D, and contour plots of $U_5(x,t)$.

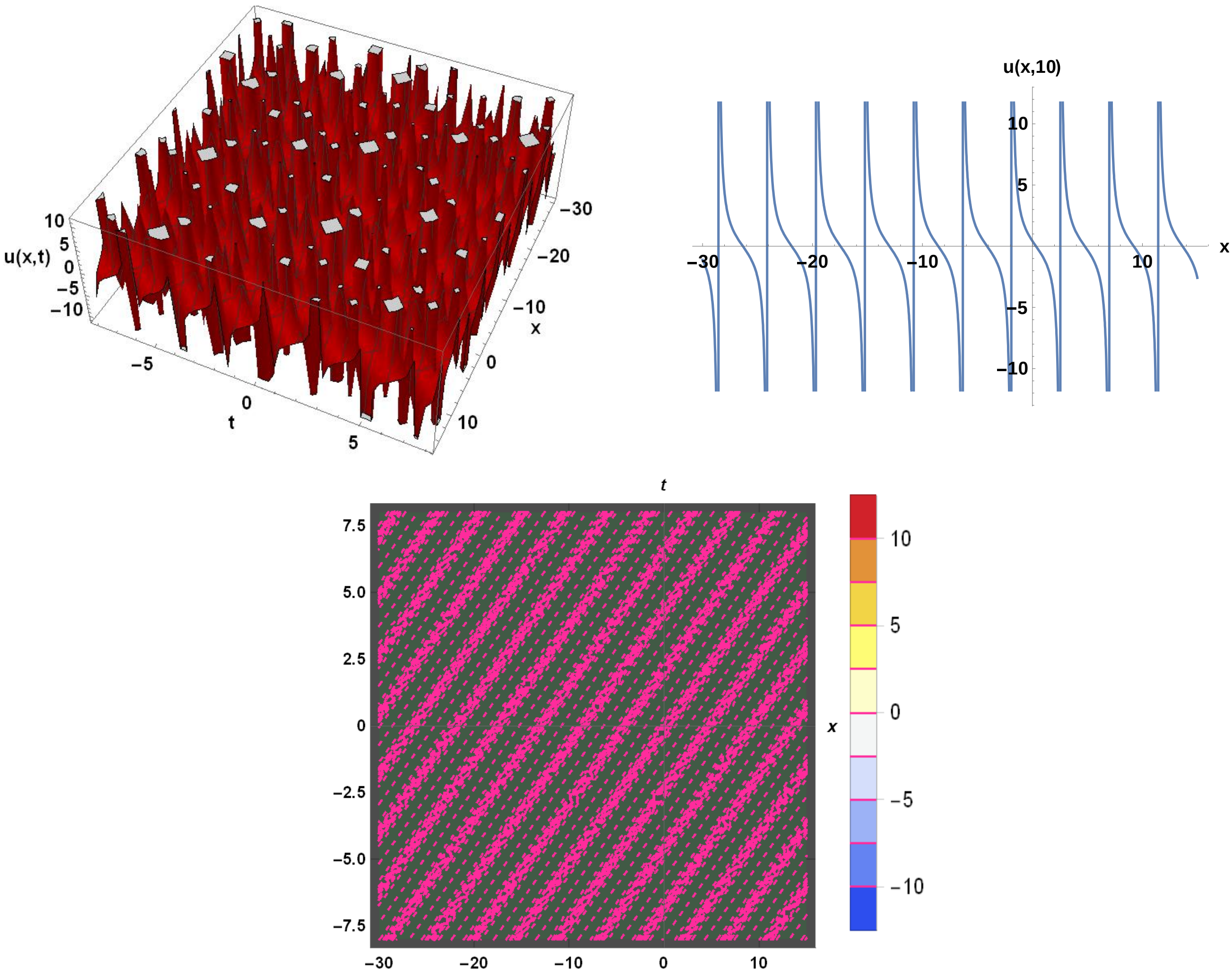

Figure 6. The solitary wave view of the 3D, 2D, and contour plots of $U_6(x,t)$.

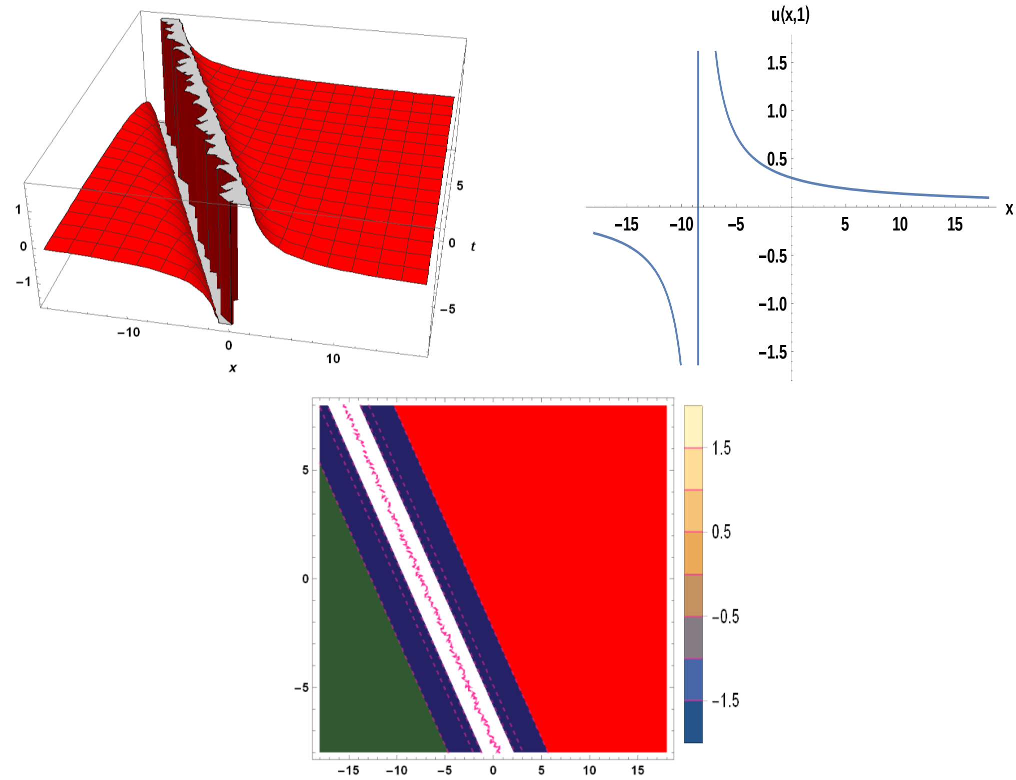

Figure 7. The solitary wave view of the 3D, 2D, and contour plots of $U_7(x, t)$.

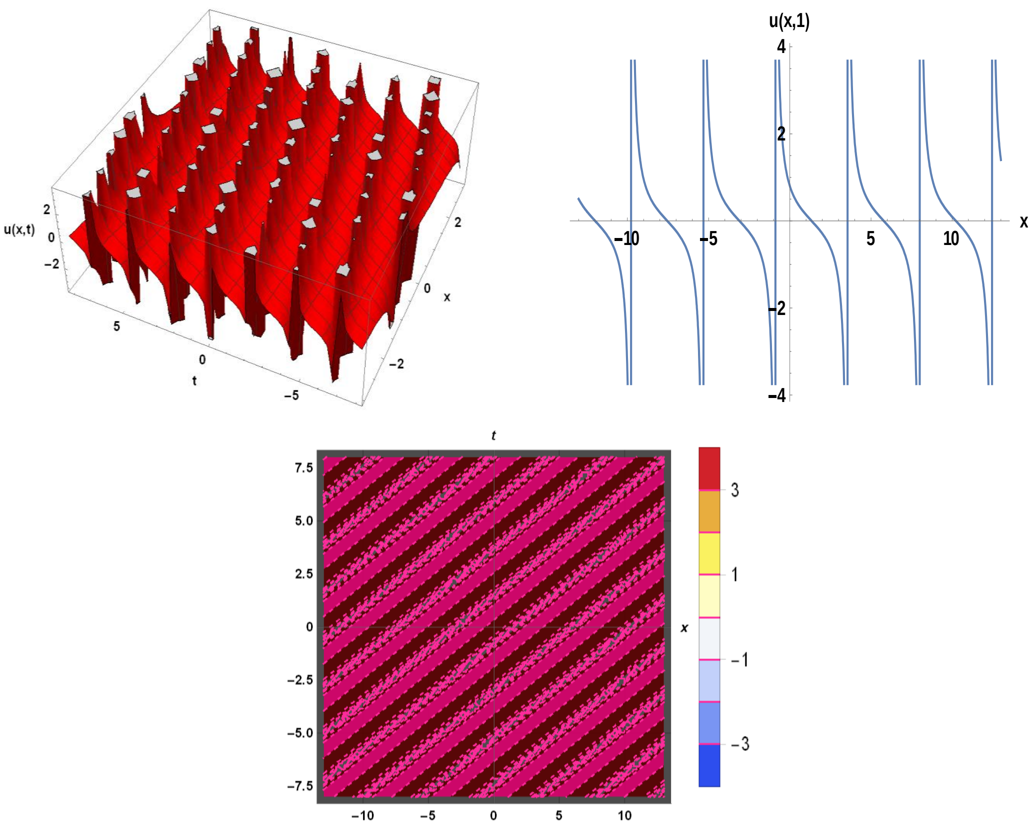

Figure 8. The solitary wave view of the 3D, 2D, and contour plots of $U_8(x, t)$.

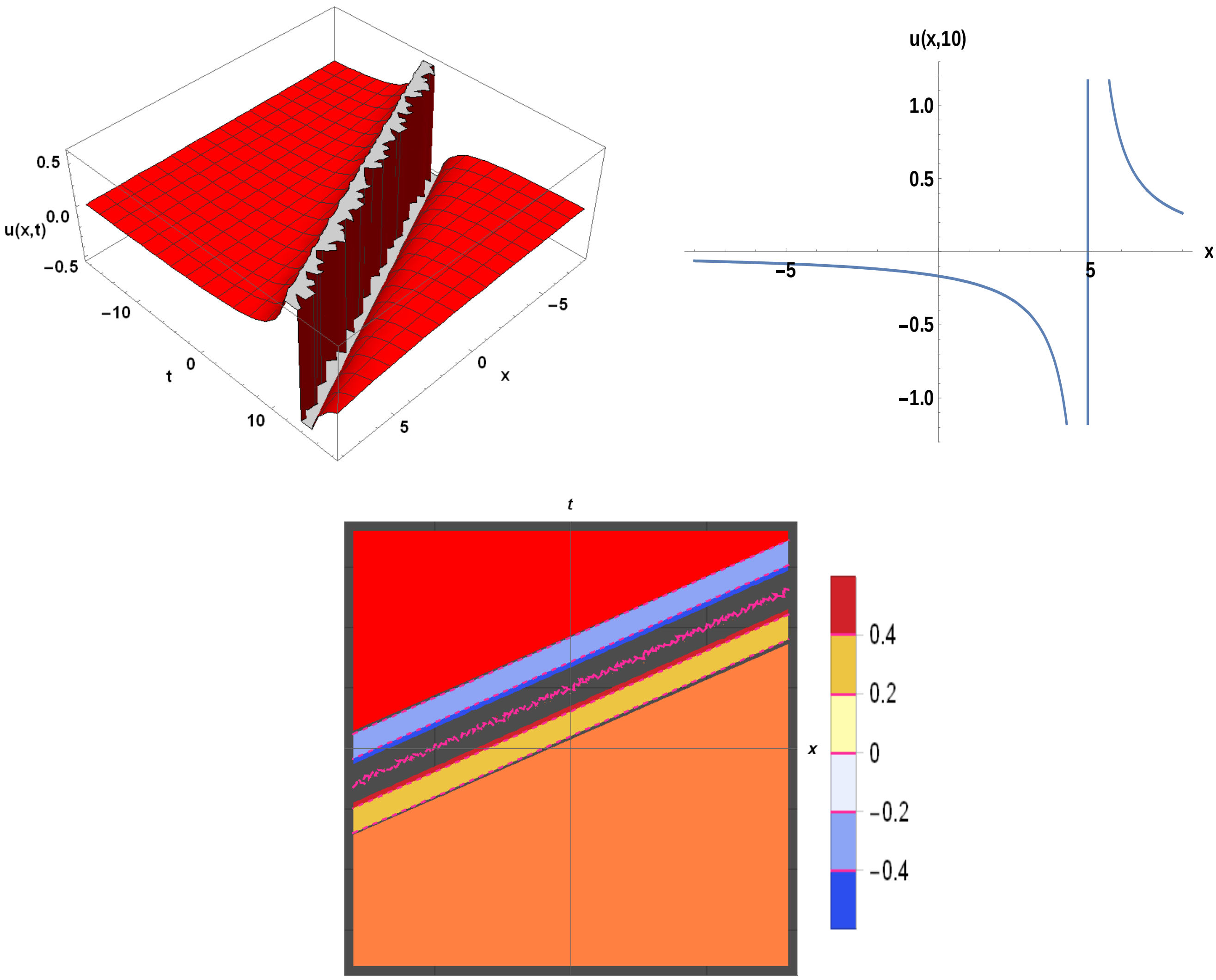

Figure 9. The solitary view of the 3D, 2D, and contour plots of $U_9(x, t)$.

Our solutions are more exact when compared with the solutions of Baskonus and Bulut [27].

5. Conclusions

The proposed approach called the generalized exp $(-\phi(\eta))$-expansion method was applied to the nonlinear DMBBM equation in this work, and many new closed form solutions were obtained. The Wolfram Mathematica 10 computer application was used to verify all of the analytical solutions developed in this study and to plot Figures 1–9 with 2D, 3D, and contour faces. We also compared the obtained solutions in this study with existing solutions in the literature. We re-derived many existing solutions in the literature where parameters were given specific values, which demonstrates the novelty of our work. Similarly, if we use Equations (10)–(16), we obtain many different and new solutions. Not only rational, but also hyperbolic and trigonometric function solutions can be obtained using this method. The generalized exp $(-\phi(\eta))$-expansion method has been shown to be a powerful tool for acquiring closed form solutions to other nonlinear partial differential equations.

Author Contributions: Formal analysis, N.A.S.; Methodology, A.; Project administration, N.A.S.; Software, E.R.E.-Z.; Supervision, J.D.C.; Funding, J.D.C.; Writing—original draft, M.S. All authors have read and agreed to the published version of the manuscript.

Funding: This work received no external fund.

Institutional Review Board Statement: Not applicable.

Informed Consent Statement: Not applicable.

Data Availability Statement: The numerical data used to support the findings of this study are included within the article.

Acknowledgments: This research was supported by Basic Science Research Program through the National Research Foundation of Korea (NRF) funded by the Ministry of Education (No. 2017R1D1A1B0-5030422).

Conflicts of Interest: The authors declare no conflict of interest.

References

1. Huang, X.; Chen, Z.; Zhao, W.; Zhang, Z.; Zhou, C.; Yang, Q.; Tian, J. An extreme internal solitary wave event observed in the northern South China Sea. *Sci. Rep.* **2016**, *6*, 30041. [CrossRef] [PubMed]
2. Yuan, C.; Grimshaw, R.; Johnson, E. The propagation of internal solitary waves over variable topography in a horizontally two-dimensional framework. *J. Phys. Oceanogr.* **2018**, *48*, 283–300. [CrossRef]
3. Pierini, S. A model for the Alboran Sea internal solitary waves. *J. Phys. Oceanogr.* **1989**, *19*, 755–772. [CrossRef]
4. Cai, S.; Xie, J. A propagation model for the internal solitary waves in the northern South China Sea. *J. Geophys. Res.* **2010**, *115*, C12074. [CrossRef]
5. Grimshaw, R.; da Silva, J.C.; Magalhaes, J.M. Odelling and observations of oceanic nonlinear internal wave packets affected by the Earth's rotation. *Ocean Model.* **2017**, *116*, 146–158. [CrossRef]
6. Chunga, K.; Toulkeridis, T. First evidence of aleo-tsunami deposits of a major historic event in Ecuador. *J. Tsunami Soc. Int.* **2014**, *33*, 55–69.
7. Shakeel, M.; Ul-Hassan, Q.M.; Ahmad, J.; Naqvi, T. Exact solutions of the time fractional BBM-Burger equation by novel (G'/G)-expansion method. *Adv. Math. Phys.* **2014**, *2014*, 181594. [CrossRef]
8. Aslam, M.N.; Akbar, M.A.; Mohyud-Din, S.T. General traveling wave solutions of the strain wave equation in microstructured solids via the new approach of generalized (G'/G)-expansion method. *Alex. Eng. J.* **2014**, *53*, 233–241. [CrossRef]
9. Yusufoğlu, E.; Bekir, A. Solitons and periodic solutions of coupled nonlinear evolution equations by using the sine-cosine method. *Int. J. Comput. Math.* **2006**, *83*, 915–924. [CrossRef]
10. Bashir, M.A.; Moussa, A.A. The $\coth_a(\xi)$ Expansion method and its application to the davey-stewartson equation. *Appl. Math. Sci.* **2014**, *8*, 3851–3868.
11. Bashir, M.A.; Alhakim, L.A. New F expansion method and its applications to modified KdV equation. *J. Math. Res.* **2013**, *5*, 83–94. [CrossRef]
12. He, J.H.; Wu, X.H. Exp-function method for nonlinear wave equations. *Chaos Solitons Fractals* **2006**, *30*, 700–708. [CrossRef]
13. Yahya, K.H.; Moussa, Z.A. New approach of generalized exp $(-\phi(\xi))$-expansion method and its application to some nonlinear partial differential equations. *J. Math. Res.* **2015**, *7*, 106–121.
14. Akbar, M.A.; Ali, N.H.M. Solitary wave solutions of the fourth order Boussinesq equation through the exp $(-\Phi\,(\eta))$-expansion method. *Springer Plus* **2014**, *3*, 344. [CrossRef]
15. Khan, K.; Akbar, M.A. Application of $\exp(-\phi(\xi))$-expansion method to find the exact solutions of modified Benjamin-Bona-Mahony equation. *World Appl. Sci. J.* **2013**, *24*, 1373–1377.
16. Fei, J.X.; Cao, W. Explicit soliton–cnoidal wave interaction solutions for the (2 + 1)-dimensional negative-order breaking soliton equation. *Waves Random Complex Media* **2020**, *30*, 54–64. [CrossRef]
17. Wang, B.H.; Wang, Y.-Y.; Dai, C.-Q.; Chen, Y.-X. Dynamical characteristic of analytical fractional solitons for the space-time fractional Fokas-Lenells equation. *Alex. Eng. J.* **2020**, *59*, 4699–4707. [CrossRef]
18. Wen, X.K.; Feng, R.; Lin, J.; Liu, W.; Chen, F.; Yang, Q. Distorted light bullet in a tapered graded-index waveguide with PT symmetric potentials. *Optik* **2021**, *248*, 168092. [CrossRef]
19. Fang, Y.; Wu, G.-Z.; Wang, Y.-Y.; Dai, C.-Q. Data-driven femtosecond optical soliton excitations and parameters discovery of the high-order NLSE using the PINN. *Nonlinear Dyn.* **2021**, *105*, 603–616. [CrossRef]
20. Raghuraman, P.J.; Shree, S.B.; Rajan, M.S.M. Soliton control with inhomogeneous dispersion under the influence of tunable external harmonic potential. *Waves Random Complex Media* **2021**, *31*, 474–485. [CrossRef]
21. Yusufoğlu, E. New solitonary solutions for the MBBM equations using Exp-function method. *Phys. Lett. A* **2008**, *372*, 442–446. [CrossRef]
22. Zayed, E.M.E.; Al-Joudi, S. Applications of an extended (G'/G)-expansion method to find exact solutions of nonlinear PDEs in mathematical physics. *Math. Probl. Eng.* **2010**, *2010*, 768573. [CrossRef]
23. Khan, K.; Akbar, M.A.; Islam, S.M.R. Exact solutions for (1 + 1)-dimensional nonlinear dispersive modified Benjamin-Bona-Mahony equation and coupled Klein-Gordon equations. *Springer Plus* **2014**, *3*, 724. [CrossRef] [PubMed]

24. Tascan, F.; Akbulut, A. Construction of exact solutions to partial differential equations with CRE method. *Commun. Adv. Math. Sci.* **2019**, *2*, 105–113. [CrossRef]
25. Yokus, A.; Sulaiman, T.A.; Gulluoglu, M.T.; Bulut, H. Stability analysis, numerical and exact solutions of the (1 + 1)-dimensional NDMBBM equation. *ITM Web Conf.* **2018**, *22*, 01064. [CrossRef]
26. Khater, M.M.A.; Nofal, T.A.; Zinadah, H.A.; Lotayif, M.S.M.; Lu, D. Novel computational and accurate numerical solutions of the modified Benjamin-Bona-Mahony (BBM) equation arising in the optical illusions field. *Alex. Eng. J.* **2021**, *60*, 1797–1806. [CrossRef]
27. Baskonus, H.M.; Bulut, H. Analytical studies on the (1 + 1)-dimensional nonlinear dispersive modified Benjamin-Bona-Mahony equation defined by seismic sea waves. *Waves Random Complex Media* **2015**, *25*, 11. [CrossRef]